UDC: 621.396.663

ANALYSIS OF LOCATION UNCERTAINTY BY TRIANGULATION IN THE PROCESS OF SPECTRUM MONITORING[1]

Dr. **Kogan V.V.** - former leading researcher of NIIDAR,

Dr. **Pavlyuk A.P.** – consultant of JSC IRCOS.

Keywords: *spectrum monitoring, direction finding, location determination, direction finding uncertainty, location uncertainty*

Introduction

Remote location of emission sources using direction finders (DFs) by triangulation is of great importance for increasing the efficiency of spectrum monitoring. The more accurate and reliable the remote location of fixed direction finders is carried out, the easier and faster it will be possible to find the desired emission source on the spot with the help of a mobile spectrum monitoring station that operatively interacts with fixed stations. At the same time, location is perhaps the most complex and time-consuming function of spectrum monitoring that the most affected by reflections of radio signals from all kinds of objects and obstacles. It is a reason that the issues of increasing the efficiency and reliability of location have been studied for many years by the Study Group 1 Spectrum Management of the Radiocommunication Sector of the International Telecommunication Union (ITU-R).

A distinctive feature of this spectrum monitoring function is the fact that, as shown in [1] and [2], the location uncertainty (LU), even the instrumental one (i.e. the minimum possible), is not a constant value, but varies significantly within the general territory covered by the location. To date, the literature does not provide a detailed methodology for calculating the instrumental LU. This article aims to fill this gap with an analysis performed many years ago.

Methodology of the instrumental LU evaluation

As noted in [1], a rigorous analytical solution to this problem for the general case of multiple direction finders is very difficult, so success largely depends on how well the approximation is applied. The following limitations are accepted in this analysis:

- an exclusively instrumental LU is analyzed, which depends entirely on the DF instrumental uncertainty of bearings, i.e. no external influences are taken into account;

[1] Unofficial translation into English of the article published in Russian by Electrosviaz № 7, 2022.

- calculations are carried out in relation to two DFs that are located closest to the desired emission source and both "see" this emission source; considering DFs in pairs, the analysis can be extended to any number of DFs in the local network;
- as a measure of the LU, the value of the major half-axis of the corresponding uncertainty ellipse is taken.

As shown in Figure 1, due to certain errors that occur during the processing of the signal received by the DF **П**, the line of the measured bearing may differ slightly from the line of the true bearing. Since several random factors can influence the result during the signal processing by the DF, the law of the distribution of the values of the angle by which the line of the measured bearing deviates can be assumed as to be the normal one, i.e.

$$p(\delta\theta) = \frac{1}{\sqrt{2\pi}\cdot\sigma_\theta}\cdot e^{-\frac{\delta\theta^2}{2\sigma_\theta^2}}\delta\theta \qquad (1)$$

Here σ_θ is the RMS of the measured angle,

$\delta\theta$ is the value of the deviation of the angle measurement result from the true one.

In DF actions, it is not the uncertainty of the angle measuring that is of greater interest, but the linear uncertainty of measuring the distance on the ground, determined by the interval between the true position of the emission source and the position of the emission source determined by DF.

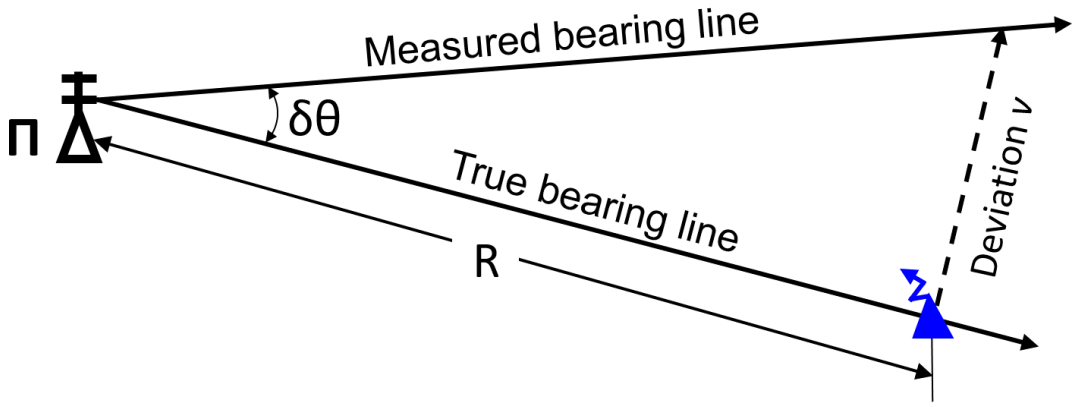

Figure 1. Bearing uncertainty

The relationship of the uncertainty of angle measurement with the distance between the points on the true and measured bearing lines for a flat Earth and the limited values of the angle measurement uncertainty (in order of several degrees) is determined by the linear equation (see Figure 1):

$$v = \delta\theta \cdot R \qquad \sigma_R = \sigma_\theta \cdot R$$

If it is necessary to take into account the influence of the Earth sphericity, the point and the angle of the bearing lines intersection should be determined using spherical geometry formulas.

The probability of a linear error v occurring at a distance R from the DF is determined by the expression:

$$p(v) = \frac{1}{\sqrt{2\pi} \cdot \sigma_\theta R} \cdot e^{-\frac{(\delta\theta R)^2}{2(\sigma_\theta R)^2}} \delta\theta R = \frac{1}{\sqrt{2\pi} \cdot \sigma_R} \cdot e^{-\frac{v^2}{2\sigma_R{}^2}} dv$$

If two DFs are tracking the same emission source, standing by distances R_1 and R_2 from each of them, respectively, then the probability of simultaneous occurrence of uncertainties with values v_1 on one DF and v_2 on the other will be determined by a two-dimensional normal distribution law:

$$p(v_1, v_2) = \frac{1}{2\pi \cdot \sigma_{R1}\sigma_{R2}} \cdot e^{-\frac{v_1{}^2}{2\sigma_{R1}{}^2} + \frac{v_2{}^2}{2\sigma_{R2}{}^2}} dv_1 dv_2 \qquad (2)$$

Here we consider the uncertainties of measuring the angle on each of the DFs to be independent, and therefore the uncertainties of estimating linear distances are also independent.

Figure 2 shows the intersection of the uncertainty sectors of the bearing lines of two DFs **П1** and **П2**. As a result, we have an LU ellipse, the dimensions of which depend on the angle of intersection of the sectors and on the probability p with which the desired emission source is located within this ellipse.

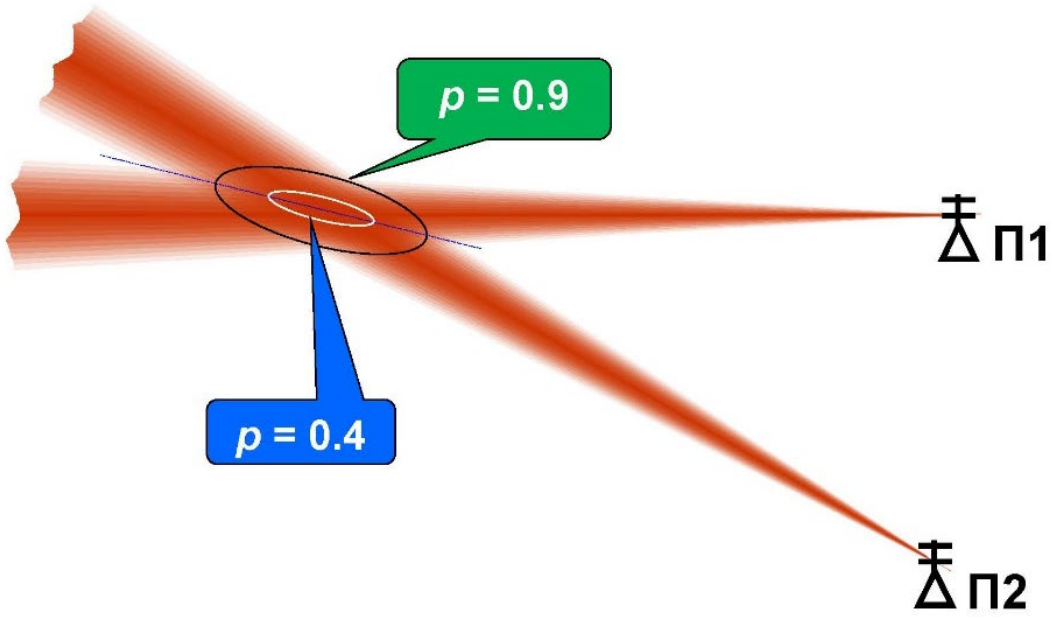

Figure 2. LU ellipse of two DFs

The LU ellipse in a general form is represented in Figure 3. If the bearing lines intersect at right angles, i.e. at $\varphi = 45$ °, the ellipse turns into a circle with minimum and equal values of the semi-axes. Depending on the relative position of the DFs, both the half-axis *A* and *B* can take a larger value.

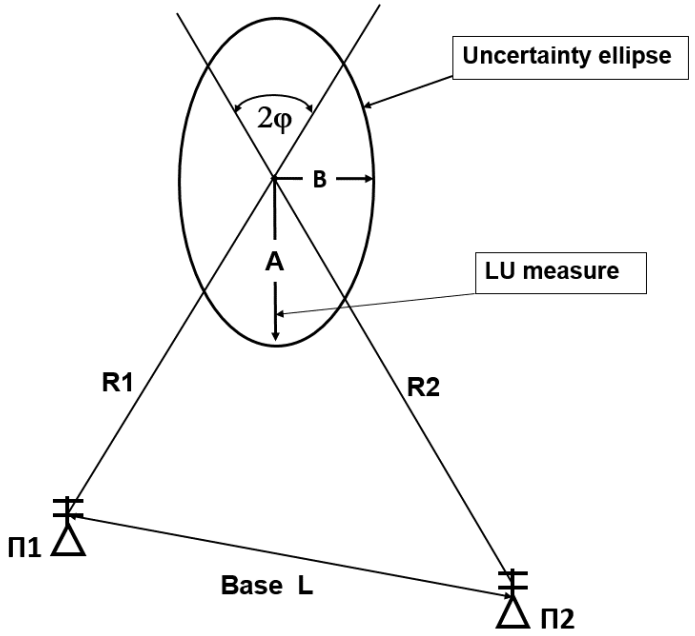

Figure 3. Parameters of the LU ellipse

Solving the oblique triangle *R1-R2-L* [3] we get:

$$\varphi = ArcTg\left\{\sqrt{\frac{(s-R_1)(s-R_2)}{s(s-L)}}\right\} \tag{3}$$

where

$$s = \frac{R_1 + R_2 + L}{2}$$

Let us rearrange formula (2) to a form more convenient for performing calculations using the following input data: distances *R1, R2, L* and the RMS of the instrumental uncertainties of both DFs: $\sigma_{\theta 1}$, $\sigma_{\theta 2}$. For this, let us consider the situational plan shown in Figure 4 with intersecting lines of two bearings, an emission source spaced from the point of intersection of the bearing lines, and an accepted coordinate system. The point of intersection of the bearing lines is the result of measurements and in general, it does not correspond to the point at which the emission source is located.

Let us introduce coordinate axes by placing the coordinate origin to the point of the bearing lines intersection. The *y*-axis is directed along the bisectrix of the intersection angle, and the *x*-axis is perpendicular to the *y*-axis. The angle between the axis and the bearing lines is denoted by φ. Let the true position of the

emission source be determined in these coordinates by a point with x and y coordinates. The distance from the true emission source to each of the bearing lines is denoted by v_1 and v_2, respectively. These are linear measurement uncertainties.

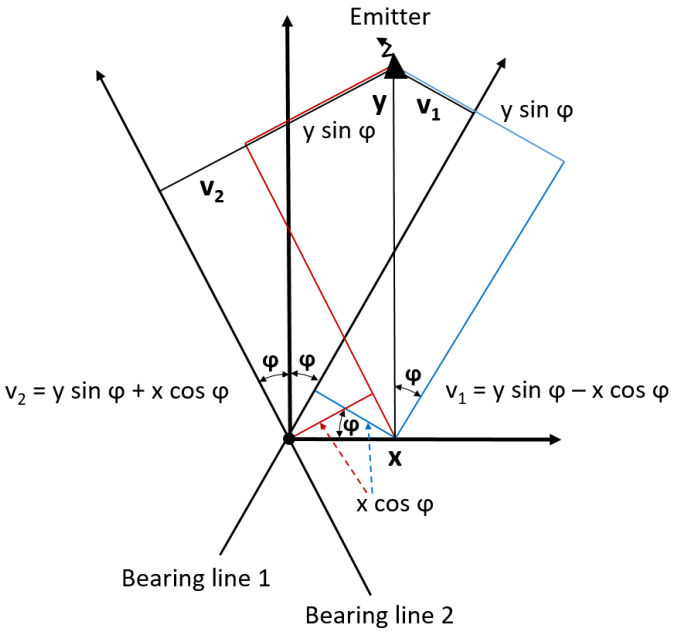

Figure 4. Situational plan

Let us express measurement uncertainties in terms of coordinates. Obviously,

$$v_1 = y \cdot \sin\varphi - x \cdot \cos\varphi \qquad v_2 = y \cdot \sin\varphi + x \cdot \cos\varphi$$

The Jacobian of the transformation J [3] is defined as follows:

$$\begin{vmatrix} v_1 \\ v_2 \end{vmatrix} = \begin{vmatrix} -\cos\varphi & \sin\varphi \\ \cos\varphi & \sin\varphi \end{vmatrix} \cdot \begin{vmatrix} x \\ y \end{vmatrix} \qquad J = \begin{Vmatrix} -\cos\varphi & \sin\varphi \\ \cos\varphi & \sin\varphi \end{Vmatrix} = \left| -2\sin\varphi\cos\varphi \right| = \sin 2\varphi$$

Substitute these expressions into the probability formula (2):

$$p(x,y) = \frac{\sin 2\varphi}{2\pi \cdot \sigma_{R1}\sigma_{R2}} \cdot e^{-\frac{(y\cdot\sin\varphi - x\cdot\cos\varphi)^2}{2\sigma_{R1}^2} - \frac{(y\cdot\sin\varphi + x\cdot\cos\varphi)^2}{2\sigma_{R2}^2}} dxdy \qquad (4)$$

Now we have obtained an expression for the probability of displacement of the true position of the emission source relative to the origin, i.e. relative to the point of the bearing lines intersection in coordinates *x0y*. It is easier to analyze uncertainties in x and y coordinates than in v_1 and v_2 coordinates.

Opening the brackets in the exponent and collect the coefficients for the variables we will get:

$$\frac{(y\sin\varphi - x\cos\varphi)^2}{2\sigma_{R1}} + \frac{(y\sin\varphi + x\cos\varphi)^2}{2\sigma_{R2}} =$$

$$= \frac{y^2\sin^2\varphi - 2xy\sin\varphi\cos\varphi + x^2\cos^2\varphi}{2\sigma^2_{R1}} + \frac{y^2\sin^2\varphi + 2xy\sin\varphi\cos\varphi + x^2\cos^2\varphi}{2\sigma^2_{R1}} =$$

$$= x^2\cos^2\varphi\left(\frac{1}{2\sigma^2_{R1}} + \frac{1}{2\sigma^2_{R2}}\right) + y^2\sin^2\varphi\left(\frac{1}{2\sigma^2_{R1}} + \frac{1}{2\sigma^2_{R2}}\right) + 2xy\sin\varphi\cos\varphi\left(-\frac{1}{2\sigma^2_{R1}} + \frac{1}{2\sigma^2_{R2}}\right)$$

$$p(x,y) = \frac{\sin 2\varphi}{2\pi\cdot\sigma_{R1}\sigma_{R2}}\cdot e^{-(a_{11}x^2 + 2a_{12}xy + a_{22}y^2)}dxdy$$

$$a_{11} = \cos^2\varphi\left(\frac{1}{2\sigma_{R1}^2} + \frac{1}{2\sigma_{R2}^2}\right) \tag{5}$$

$$a_{22} = \sin^2\varphi\left(\frac{1}{2\sigma_{R1}^2} + \frac{1}{2\sigma_{R2}^2}\right) \tag{6}$$

$$a_{12} = \sin\varphi\cdot\cos\varphi\cdot\left(\frac{1}{2\sigma_{R2}^2} - \frac{1}{2\sigma_{R1}^2}\right) \tag{7}$$

The magnitude of the φ angle is determined by the formula (3).

Note that the linear measurement uncertainties are correlated. The degree of correlation is determined by a coefficient a_{12} depending on the angle of the bearing lines intersection. There is no correlation at $a_{12} = 0$ (when bearing line intersection angle is 90°). If this angle approaches zero, then the two-dimensional normal distribution law degenerates into a one-dimensional one.

It is easy to see that the probability depends only on the exponent. If *x* and *y* change, outlining a line at the *x0y* plane, so that the exponent remains constant, then the probability at this line will remain constant. The exponent is a quadratic form, and the line of constant probability here is an ellipse. The equation of constant probability is the equation of an ellipse given in the form (the constant *K* in the right part of the equation can be arbitrary):

$$\frac{(Y\cdot\sin\varphi - X\cdot\cos\varphi)^2}{2\sigma_{R1}^2} + \frac{(Y\cdot\sin\varphi + X\cdot\cos\varphi)^2}{2\sigma_{R2}^2} = \frac{K^2}{2} \tag{8}$$

In (8), the constant is chosen so that when $K = 1$ and the bearing lines intersect at right angles, the dimensions of the semi-axes of the ellipse are equal to the RMS along corresponding coordinates.

Integrating the two-dimensional probability density (4) over the area bounded by the ellipse (8), we obtain the probability that the true position of the emission source is located within the *x0y* plane bounded by this ellipse.

Each value of K corresponds to its own ellipse size and its own probability. If K is increased, the dimensions of the ellipse increase. The area covered by the ellipse becomes larger. The area of uncertainty with respect to the position of the emission source, outlined by an ellipse, increases. At the same time, the probability that the emission source is located within this ellipse increases. If we want to increase the probability that the emission source, we are interested in, was within the ellipse, we must increase the size of the ellipse. Thus, requiring an increase in the probability of estimating the location, we inevitably have to increase the uncertainty zone – to increase the size of the ellipse. This is why the ellipse is called the uncertainty ellipse or the LU ellipse.

The probability of finding an emission source inside the LU ellipse is determined by the Rayleigh distribution. The probability values for some values of K are given in Table 1.

Table 1

Probability	0.39	0.5	0.6	0.63	0.7	0.8	0.9	0.95
K	1.00	1.18	1.35	1.41	1.55	1.79	2.15	2.45

When estimating the direction finding conditions for the entire monitoring zone, it is more convenient that each point of this zone is characterized by a single digit. Characterization of each point of the zone with three digits (the slope of the ellipse axes and their dimensions) presents certain inconveniences for a generalized assessment of the monitoring quality of the entire zone. When choosing a characteristic number, the main monitoring task should be taken into account.

The determination of bearings by fixed stations is carried out for the proper orientation of mobile spectrum monitoring stations. The main limitation when locating the emission source by mobile stations is the possible search range relative to the point of the bearing lines intersection. Since the maximum uncertainty is oriented along the major axis of the ellipse, it is possible to set the dimensions of the uncertainty area in the form of a circle with a radius equal to the length of the major semi-axis of the uncertainty ellipse. By choosing, for example, a coefficient $K = 2.15$ for calculating the dimensions of the major semi–axis of the ellipse, we guarantee that even in the worst case - the displacement of the true position of the emitter along the large axis of the ellipse - the probability that this displacement will not go beyond the ellipse will be equal 0.9. In other directions, the displacement with the specified probability will be significantly less. Thus, such an assessment is an estimation with a margin and can be considered as to be guaranteed.

The determination of the uncertainty ellipse parameters is carried out taking into account the expressions (5,6,7) by to the following formulas for calculating the values of the uncertainty ellipse semi-axes:

$$A = \sqrt{\frac{K^2}{2\lambda_1}} \qquad B = \sqrt{\frac{K^2}{2\lambda_2}} \tag{9}$$

where

$$\lambda_1 = \frac{(a_{11} + a_{22}) - \sqrt{(a_{11} - a_{22})^2 + 4a_{12}^2}}{2} \qquad \lambda_2 = \frac{(a_{11} + a_{22}) + \sqrt{(a_{11} - a_{22})^2 + 4a_{12}^2}}{2}.$$

The desired LU is equal to the maximum value (*A, B*).

Application of the analysis results

As follows from the above formulas, the LU significantly depends on the magnitude of the angle of the bearing line intersection of two DFs. Since the intersection angles will change for different points of the terrain, the values of the LU will draw a certain figure on the terrain. An example of such a figure (the first of the 10 figures presented in [2]) is shown in Figure 5.

Here we show the distribution of the LU values over the territory (absolutely smooth Earth) for two direction finders, of which the right one provides 1.5 times less DF uncertainty than the left one. Fragment (b) shows the central part of the figure. In two small rounded zones indicated by green where the bearing lines intersect at angles close to 90 °, the LU takes the smallest values (0.015 relative units according to the color palette shown on the right). As we move away from the DFs with a corresponding decrease in the intersection angles the values of the LU, represented by zones of different colors, consistently increase to relative values of 0.9, i.e. 60 times greater than the minimum value of the LU in this example. In [2], for the first time, the distributions of LU values obtained from calculations over the territory for 10 different placement options from 2 to 12 DFs were analyzed in detail.

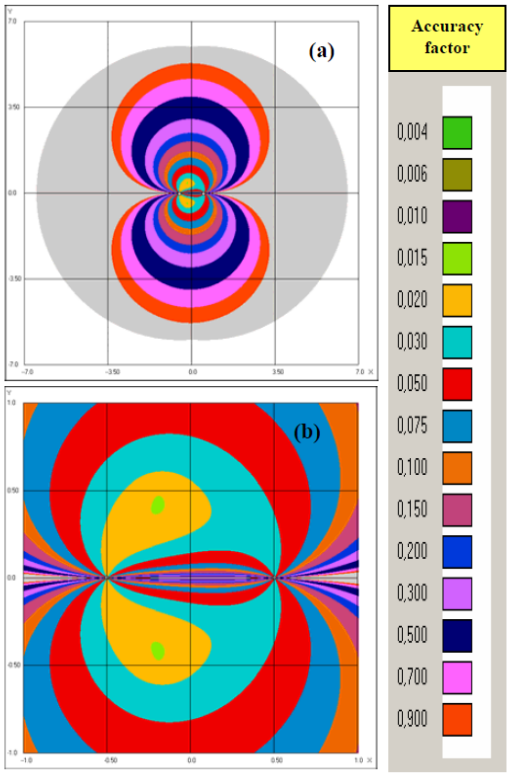

Figure 5. Distribution of LU across the territory in relative measurement values

Since the first publications on this topic [1] and [2] were planned in English, after consultations with English-speaking specialists in the field of spectrum monitoring, the images obtained of the distribution of LU across the territory were called "Location coverage templates" and were later translated into Russian as "Шаблоны охвата местоопределением", as used in the publication [4]. In this, as well as in many other publications, for example in [5], data on LU distribution are already given in absolute units. As an example, Figure 6 reproduces one of the figures given in [4]. It shows a densely populated area, where three DFs C1 – C3 are placed, and a location coverage template provided by these three DFs. The LU values are distributed over a large number of multi-colored gradations from 10 m to 10 km on the palette presented at the right of the map. The gradations not used in this particular case along the edges of the palette are combined so as not to complicate the perception of the gradations represented by the template.

As can be seen from the template, the minimum value of the LU from 100 to 200 m is achieved in four rounded zones in the central part of the template, where the bearing lines from these three DFs intersect at angles close to 90°. The maximum LU values at the edges of the template in this case correspond to a gradation from 2 to 4 km (dark brown one). Outside the outer boundaries of the colored zones, starting from the green zone of 0.4 – 0.6 km, DF is not provided due to a decrease in field strength below the threshold value set for DF in section 6.8 of the ITU Handbook on Spectrum Monitoring [6]. Calculations of radio wave propagation conditions were carried out taking into account the actual topography of the area.

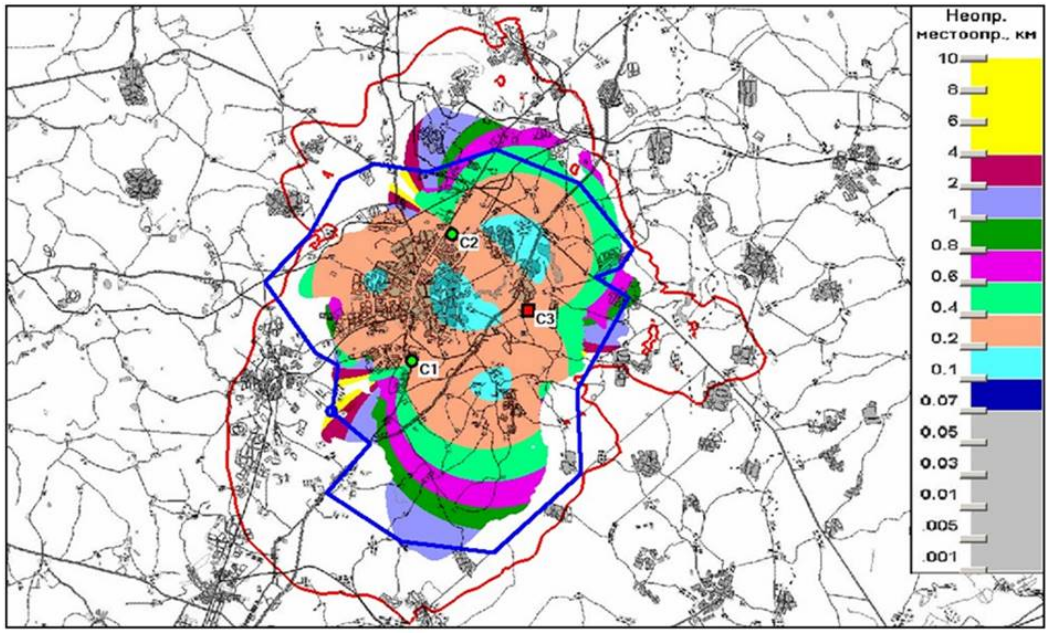

Figure 6. The LU template on a real terrain

Knowledge of the LU distribution over the terrain makes it possible to optimize the placement of fixed DFs to ensure the greatest efficiency of remote location determination. Therefore, the assessment of the LU distribution across the

territory is an essential element of the spectrum monitoring network planning procedure. The corresponding methodology, firstly proposed in [1], was later included in section 6.8 of the ITU Handbook on Spectrum Monitoring [6] and in section 3 of the ITU-R Report SM.2356-2 [7].

Implementing this methodology, in the early 2000s a fairly advanced software was created, called "Monitoring Network Planning and Optimization Tool" (MN-POT), the principles of which are presented in [8] and in Annex 5 to the ITU Handbook [9]. In the early 2010s, even more advanced software was created (although based on the same principles), which was called "Spectrum Monitoring Coverage Analyzer" (RMCA). The main characteristics of this software are presented on the Website *www.pavlyuk.com* in the RMCA SOFTWARE section. The site also presents a selection of publications on the subject of direction finding and location determination. The results of calculations performed using RMCA software were included in section 3 of the Report ITU-R SM.2356-2 [7]. From other publications on this topic, it can be noted [10]. RMCA software has been successfully used in a number of ITU technical assistance projects conducted in developing countries on the subject of planning and optimizing their spectrum monitoring networks. Publication [11] demonstrates the effectiveness of using this software at mobile spectrum monitoring stations to visualize their activities in conjunction with fixed stations.

Conclusion

The results of calculations performed based on the conducted LU analysis have been widely used both in our country and abroad. The publication of the details of this analysis should contribute to further progress in this rather complex field of activity.

References

1. **Kogan V.V., Pavliouk A.P.** Methodology of spectrum monitoring networks planning // Proceedings of the Seventeenth International Wroclaw Symposium and Exhibition on Electromagnetic Compatibility, EMC-2004. - Wroclaw, Poland, 2004. (A copy is available at www.pavlyuk.com.)
2. **Kogan V.V., Pavliouk A.P.** Analysis of location coverage templates in spectrum monitoring // Proceedings of the Seventeenth International Wroclaw Symposium and Exhibition on Electromagnetic Compatibility, EMC-2004. - Wroclaw, Poland, 2004. (A copy is available at www.pavlyuk.com.)
3. **Bronshteyn I.N., Semesendyaev K.A**. Catalog of mathematics for engineers and students of universities // State Publishing House of Technical and Theoretical Literature. - Moscow. - 1957. (In Russian)
4. **Krutova O.E., Pavlyuk A.P., Plossky A.Yu.** Planning and optimization of spectrum monitoring networks in VHF/UHF range // Electrosviaz. - 2009. - №5. (In Russian, translation into English is available at www.pavlyuk.com.)

5. **Krutova O.E., Pavlyuk A.P., Plossky A.Yu.** Improving characteristics of the Russian spectrum monitoring network in the RF range // Electrosviaz. - 2008. - №9. (In Russian, translation into English is available at www.pavlyuk.com.)

6. **International Telecommunication Union.** Handbook on Spectrum Monitoring. - Geneva, Radiocommunication Bureau. - 2011.

7. **Report ITU-R SM.2356-2** (06/2018). Procedures for planning and optimization of spectrum-monitoring networks in the VHF/UHF frequency range.

8. **Krutova O.E., Kogan V.V., Pavliouk A.P.** Advanced software for planning and optimization of spectrum monitoring networks // Proceedings of the Sixth International Symposium on Electromagnetic Compatibility and Electromagnetic Ecology, EMC'2005. - Saint-Petersburg, Russia, 2005. (A copy is available at www.pavlyuk.com.)

9. International Telecommunication Union. Handbook on Computer-aided Techniques for Spectrum Management (CAT) - Geneva, Radiocommunication Bureau. - 2015.

10. **Krutova O.E., Luther W., Pavlyuk A.P.** Analysis of location characteristics of the USA HF international spectrum monitoring network using new software // Proceedings of the Eighteenth International Wroclaw Symposium and Exhibition on Electromagnetic Compatibility, EMC-2006. - Wroclaw, Poland, 2006. (A copy is available at www.pavlyuk.com.)

11. **Bondarenko K.V., Krutova O. E., Pavlyuk A. P.** Visualization of coverage areas of VHF/UHF spectrum monitoring stations in the course of their routine operations // Proceedings of the Nineteenth International Wroclaw Symposium and Exhibition on Electromagnetic Compatibility, EMC-2008, - Wroclaw, Poland, 2008. (A copy is available at www.pavlyuk.com.)
